Liquid Crystals
Publication details, including instructions for authors and subscription information:
http://www.informaworld.com/smpp/title~content=t713926090

Electrically controlled birefringence colours in deformed helix ferroelectric liquid crystals

Gurumurthy Hegde[a]; Peizhi Xu[a]; Eugene Pozhidaev[ab]; Vladimir Chigrinov[a]; Hoi Sing Kwok[a]
[a] The Hong Kong University of Science and Technology, Kowloon, Hong Kong [b] P.N. Lebedev Physical Institute, Moscow 119991, Russia

To cite this Article Hegde, Gurumurthy , Xu, Peizhi , Pozhidaev, Eugene , Chigrinov, Vladimir and Kwok, Hoi Sing(2008) 'Electrically controlled birefringence colours in deformed helix ferroelectric liquid crystals', Liquid Crystals, 35: 9, 1137 — 1144
To link to this Article: DOI: 10.1080/02678290802398226
URL: http://dx.doi.org/10.1080/02678290802398226

Liquid Crystals,
Vol. 35, No. 9, September 2008, 1137–1144

Taylor & Francis
Taylor & Francis Group

Electrically controlled birefringence colours in deformed helix ferroelectric liquid crystals

Gurumurthy Hegde[a], Peizhi Xu[a], Eugene Pozhidaev[ab], Vladimir Chigrinov[a]* and Hoi Sing Kwok[a]

[a]*The Hong Kong University of Science and Technology, Clear Water Bay, Kowloon, Hong Kong;* [b]*P.N. Lebedev Physical Institute, Leninsky pr.53, Moscow 119991, Russia*

(Received 19 July 2008; accepted 8 August 2008)

A short helix pitch (p_0=0.45 μm) ferroelectric liquid crystal (FLC) mixture was found to provide four electrically switched birefringence colours: blue, green, yellow and red. The contrast ratios of the birefringence colours were measured as functions of both driving voltage amplitude and frequency. The FLC mixture, which had a relatively high birefringence, $\Delta n \geq 0.2$, was controlled by a voltage less than 5 V. A simple model is proposed, which was confirmed by experiments. A possible application is discussed in field-sequential colour displays, where fast switching times are required.

Keywords: passively addressed FLC display; grey scale; memory; multistability; electro-optics

1. Introduction

Recently, colour-sequential liquid crystal displays (LCDs) have become a hot topic of research (*1–5*) since they require no colour filter; thus, display primary colours are applied in a temporal sequence. Colour-sequential LCDs provide the potential to realise high-definition displays based on the current level of semiconductor technology, which are difficult to achieve using traditional colour filter LCD technology since each single pixel consists of three sub-pixels. Furthermore, the brightness of colour-sequential LCDs is much higher than that of conventional LCDs with colour filters. To achieve this, very fast response times are necessary to avoid the flicker phenomenon (*6*). An obvious contender for this application are ferroelectric liquid crystals (FLCs) since they have fast response times in ths sub-millisecond range (*7, 8*). Recently, Xu *et al.* demonstrated a colour-sequential display based on stacked bistable ferroelectric LCDs (*9*). In this configuration, they used three stacked FLC cells to produce colours. Here, we improve the present technology by eliminating two cells. In other words, our device is constructed with one FLC cell and birefringence colour is controlled by a relatively small voltage.

Application of an external electric field to a FLC results in deformation of the FLC helix and is manifest in an electro-optical response that was first reported by Meyer *et al.* in 1975 (*10*). This special type of electro-optical effect in FLCs with a short helix pitch, $p_0 < 1$ μm, and rather large tilt angle ($\theta > 30^\circ$) was designated the deformed helix ferroelectric (DHF) effect (*11*). In a surface-stabilised FLC cell, the helix pitch of the FLC mixture is typically greater than the thickness of the cell, which results in an unwinding of the helix from surface interactions with the cell walls (*12*). In contrast to this, a DHF helix pitch is 5–10 times smaller than the thickness of the LC layer. This allows the helix to be retained within the cell boundaries (*13*). The DHF effect has been studied extensively by a number of researchers (*14–18*). One of the main features of the DHF effect is the dependence of the effective birefringence, Δn_{eff}, of the FLC cell on applied voltage amplitude, V, and frequency, f (*12, 19*). Electrically controlled birefringence of the FLC cell is an origin of the electrically controlled colour switch (*19, 20*).

The present study demonstrates that four different colours can be obtained due to variation of the applied voltage amplitude at fixed frequency, whereas five different colours are possible owing to a change of the frequency while the voltage amplitude is fixed. This investigation provides a new path for creation of a very simple field-sequential colour displays by eliminating colour filters, which were a serious drawback in earlier generation displays.

2. Theory

The geometry of an FLC cell exhibiting the DHF effect is shown in Figure 1. The polariser on the first substrate makes an angle, β, with the helix axis (z-axis) and the analyser is crossed with respect to the polariser. The FLC layers are perpendicular to the substrates and the cell gap is much larger than the helix pitch. When an electric field is applied, the polarisation, P_s, of the chiral smectic C (SmC*) phase is reversed and FLC director rotates around

*Corresponding author. Email: eechigr@ust.hk

ISSN 0267-8292 print/ISSN 1366-5855 online

DOI: 10.1080/02678290802398226
http://www.informaworld.com

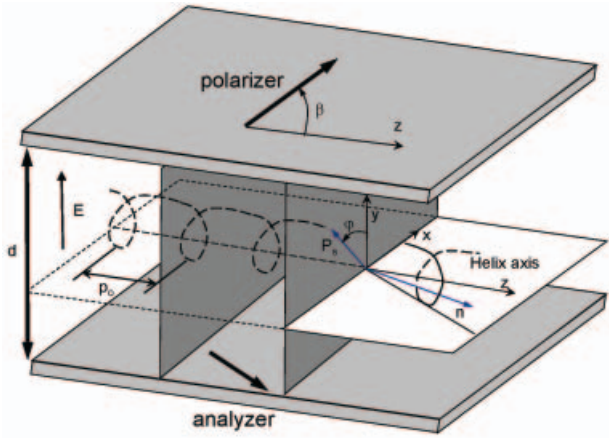

Figure 1. The location of polariser, analyser, the normal of SmC* layer (z-axis) and director. The analyser is crossed to the polariser. The normal of the SmC* layer (z-axis) is placed at an angle β to the polariser. The director of the liquid crystal rotates around the z-axis with cone angle θ_o.

the z-axis with a cone angle of $2\theta_o$. The dynamics of the FLC director in an electric field, E, smaller than the unwinding field, E_u, can be described as follows (*21*):

$$\gamma_\varphi \frac{\partial \varphi}{\partial t} + P_s E \sin \varphi + K\nabla^2 \varphi = 0, \tag{1}$$

where

$$E_u = \frac{\pi^2}{16}\frac{K_{22} q_0^2}{P_s}. \tag{2}$$

$2\pi/q_0$ is the pitch of the helicoid and depends in general on temperature (*21*), φ is the rotation angle (FLC phase during rotation) (*22*), γ_φ is the rotational viscosity, P_s the spontaneous polarisation, E the applied electric field and K the FLC elastic constant.

For the equilibrium state, the temporal relaxation term can be eliminated. Since $\varphi(z)$ is dependent on the z-direction only, Equation (1) becomes

$$P_s E \sin \varphi + K\frac{\partial^2 \varphi}{\partial z^2} = 0. \tag{3}$$

The solution of $\varphi(z)$ is given by the sum of a uniform distortion $\varphi_0(z)$ and a perturbation $\varphi_1(z)$:

$$\begin{aligned}\varphi(z) &= \varphi_0(z) + \varphi_1(z) \\ &= q_0 z + \frac{P_s E}{K q_0^2}\sin q_0 z,\end{aligned} \tag{4}$$

where $|P_s E| << K{q_0}^2$, which means $|\varphi_1| << |\varphi_0|$, when $E \updownarrow E_u$.

When the dynamic case is considered, the temporal influence only affects the perturbation part, φ_1. The solution for φ is similar to that in equilibrium state but with different φ_1. Given the solution structure of $\varphi(z)$, the dynamic form of Equation (1) can be rewritten as

$$\gamma_\varphi \frac{\partial(\varphi_0+\varphi_1)}{\partial t} + P_s E \sin(\varphi_0+\varphi_1) + K\frac{\partial^2(\varphi_0+\varphi_1)}{\partial z^2} = 0. \tag{5}$$

Equation (5) can be further simplified to

$$\gamma_\varphi \frac{\partial \varphi_1}{\partial t} + P_s E \sin \varphi_0 + K\frac{\partial^2 \varphi_1}{\partial z^2} = 0. \tag{6}$$

Assume φ_1 has the form

$$\varphi_1(z,t) = \sin q_0 z f(t). \tag{7}$$

Thus, Equation (6) can be solved for small angle, φ_1:

$$\varphi_1 = \frac{P_s E}{K q_0^2}[1 - \exp(-t/\tau)]\sin q_0 z, \tag{8}$$

where $\tau = \frac{\gamma_\varphi}{K q_0^2}$.

Thus,

$$\varphi = \varphi_0 + \varphi_1 = q_0 z + \frac{P_s E}{K q_0^2}\sin q_0 z[1 - \exp(-t/\tau)]. \tag{9}$$

If the electric field, E, is only a function of the amplitude of the applied voltage, the rotation angle, φ, can be easily determined over the pitch. If the electric field is also dependent on the frequency of the applied field, the solution of Equation (6) becomes:

$$\begin{aligned}\varphi = q_0 z - \frac{\sin q_0 z}{1+\omega^2\tau^2}\frac{P_s E_o}{K q_0^2} \\ [\tau\omega[\exp(-t/\tau) - \cos \omega t] + \sin \omega t],\end{aligned} \tag{10}$$

where we assume a harmonic electric field, $E = E_o \sin \omega t$.

However, the frequency-dependent solution is limited in application due to its intrinsic constraints. In Equation (10), to fulfil the condition $|\varphi_1| << |\varphi_0|$, the following relation should be satisfied:

$$\frac{1}{\omega^2\tau^2}\frac{P_s E_o}{K q_0^2}\tau\omega \ll 1, \tag{11}$$

which results in a limitation for frequency

$$\omega \gg \frac{P_s E_o}{\gamma_\varphi}. \tag{12}$$

For an ordinary case where $P_s = 100\,\mathrm{nC\,cm^{-2}}$, $E_o = 3\,\mathrm{V\,\mu m^{-1}}$, $\gamma_\varphi = 200\,\mathrm{mPa\,s}$, the frequency limit is $1.5 \times 10^4\,\mathrm{rad\,s^{-1}}$ (i.e. 2.4 kHz).

When the rotation angle $\varphi(z,t)$ is known, the memorised light transmission level, I, can be derived accordingly (*21*).

$$I = \langle \sin^2(2(\beta - \alpha)) \sin^2\left(\frac{\pi d}{\lambda} \Delta n_{eff}\right) \rangle \qquad (13)$$

where $<>$ mean averaging over the helix pitch and β is the angle between the normal of the SmC* layer and the polariser,

$$\alpha = \arctan(\tan\,\theta \cos\,\varphi(z,t)) \qquad (14)$$

is the angle between the projection of the optical axis on the polariser plane and the normal of SmC* layer and Δn_{eff} is the effective birefringence

$$\Delta n_{eff} = \frac{n_\parallel n_\perp}{\left[n_\perp^2 + \left(n_\parallel^2 - n_\perp^2\right)\sin^2\,\theta\,\sin^2\,\varphi(z,t)\right]^{1/2}} - n_\perp. \qquad (15)$$

Figure 2 shows the simulated spectra for different applied voltages. From the spectra, four colours, i.e. blue, green, yellow, and red, have been produced by applying four different voltages.

Figure 3 shows the simulated spectra for different frequencies of an applied electric field. Due to the limitation of the model, only spectra of a high-frequency electric field are simulated. From the spectra, two colours, i.e. cyan and blue, have been produced by applying, respectively, a 10 kHz and 250 kHz electric field with an amplitude of 15 V.

3. Experimental

Sulfonic azo-dye SD-1 (*23*) was dissolved in *N*,*N*-dimethylformamide (DMF) at a concentration of 0.4% (chemical structure of SD-1 is shown in Figure 4). An optimal (about 3–5 nm corresponding to ~0.4%) azo-dye layer thickness that provides the highest contrast ratio of the FLC display cells was found previously (*24*).

The solutions were spin-coated onto ITO electrodes at 3500 rpm and dried at 100°C for 10 min and 140°C for 20 min to remove any DMF present in the substrates. UV light was irradiated onto the photo-aligned surface of the film using a super-high-pressure Hg lamp through an interference filter at 365 nm and a polarising filter. The exposure time for UV irradiation was 90 min since at this time it attains a saturation level (*24*). The light intensity irradiated on the surface of the film was $3\,\mathrm{mW\,cm^{-2}}$ for

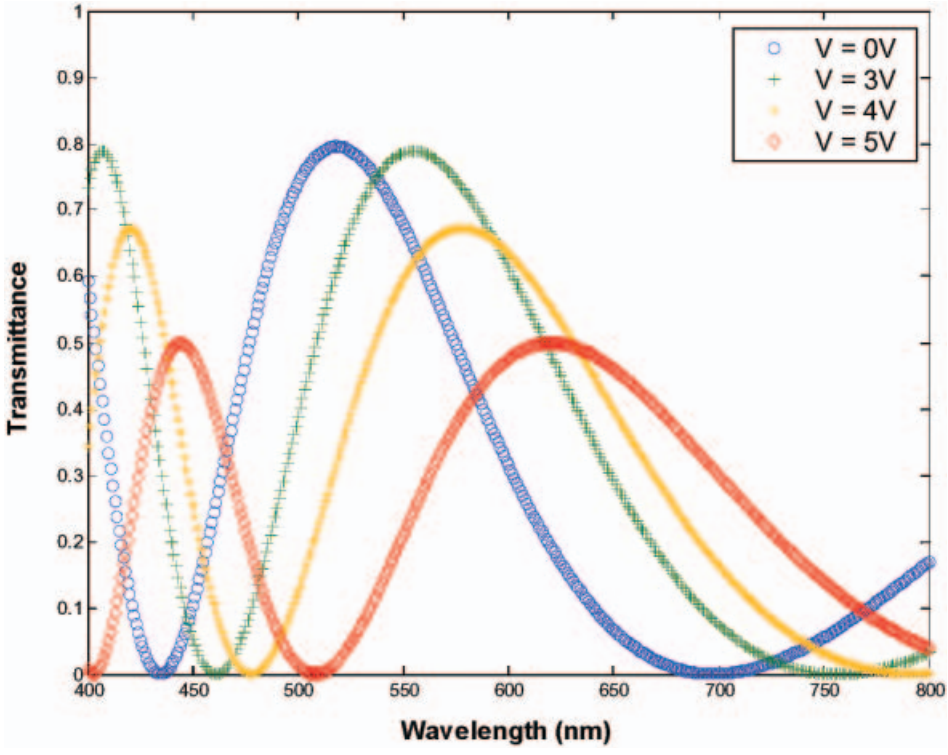

Figure 2. Simulated spectra for different applied voltage showing different wavelengths, which correspond to, namely, blue, green, yellow and red.

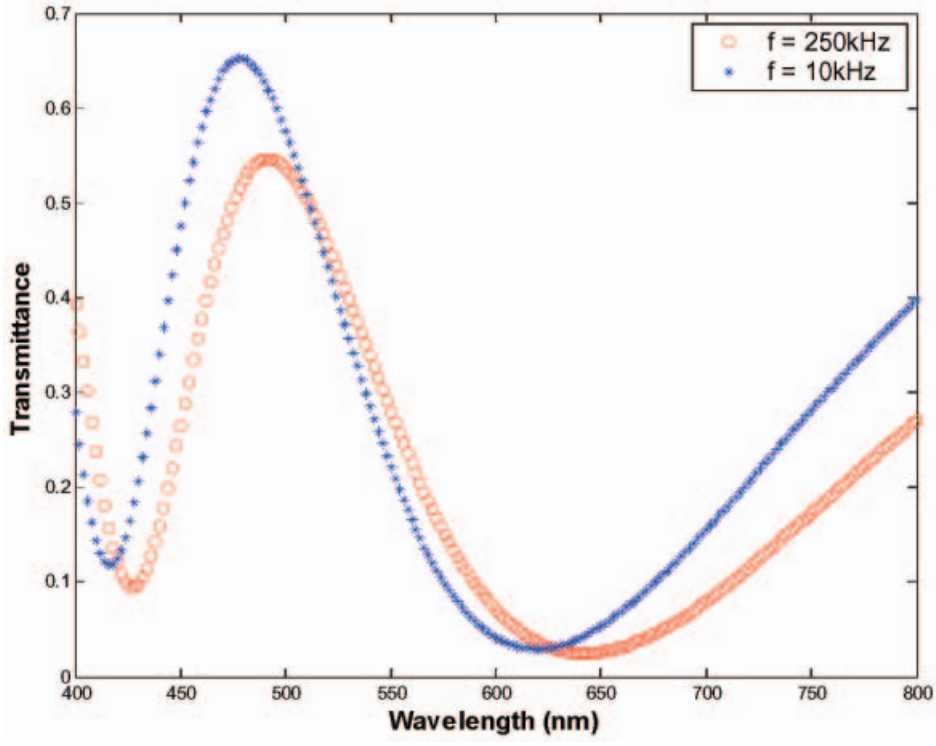

Figure 3. Simulated spectra for different frequency of applied electric field.

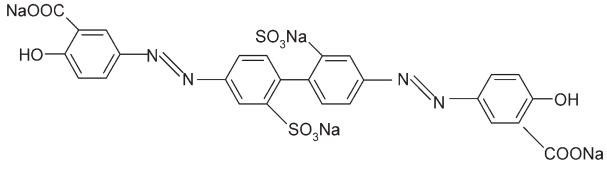

Figure 4. Chemical structure of the photoaligning azo dye, SD-1.

polarised light. The best FLC alignment quality was obtained under asymmetric boundary conditions (*24–26*), when only one ITO surface of FLC cells was prepared with the SD-1 layer, whereas another ITO surface was simply washed with DMF and covered with 5 µm diameter calibrated spacers. Thus, after assembling the FLC cells, the asymmetric boundary conditions of the FLC layer were obtained (see Figure 5).

The FLC mixtures used were FLC EPOD-08 and FLC-404 obtained from the P.N. Lebedev Physical Institute of the Russian Academy of Sciences, Moscow. These FLCs have a short helix pitch ($p_0 \sim 0.45\,\mu m$) and possess high birefringence ($\Delta n \geqslant 0.2$). FLC EPOD-08 has a spontaneous polarisation of $P_s \sim 120\,nC\,cm^{-2}$ and tilt angle $\theta \sim 30^\circ$ at room temperature. The phase transition sequence of this mixture is:

Cr 0°C SmC* 81°C SmA* 89°C I.

The FLC-404 mixture has a spontaneous polarization of $P_s \sim 230\,nC\,cm^{-2}$ and tilt angle $\theta \sim 33^\circ$ at room temperature. The phase transition sequence of this mixture is:

Cr 5°C SmC* 51°C SmA* 87.5°C I.

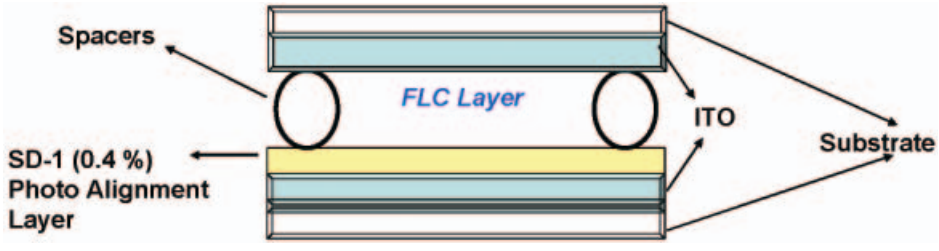

Figure 5. Configuration of the asymmetric cell; the azo dye concentration used was 0.4%.

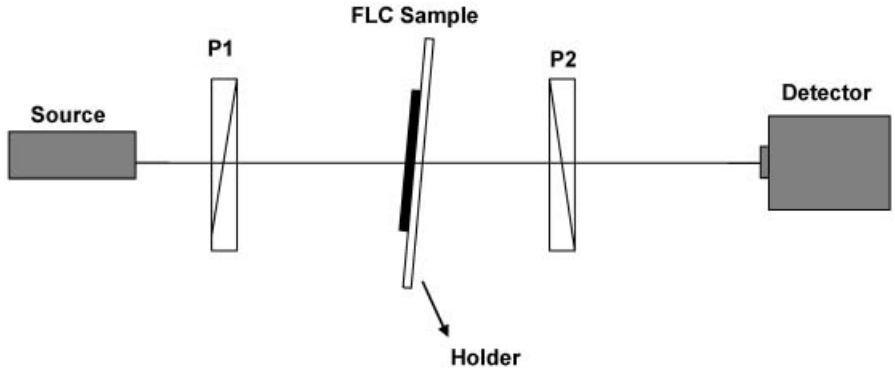

Figure 6. Experimental set-up used for this study. P1 and P2 are the polariser and analyser, respectively. The FLC cell was kept at an angle of around 45° to obtain maximum contrast for blue colour.

Because of the short helix pitch and high birefringence, both mixtures provide four electrically controlled switched birefringence colours under the action of an electric field.

The schematic diagram in Figure 6 shows the experimental set up used in this experiment. The cell was kept at 45° because in this configuration it gave maximum contrast for blue colour. The cell was kept between crossed polarisers and light transmission spectra were measured using a DT-MINI-2-GS instrument with a UV–visible–NIR light source obtained from Ocean Optics, which can measure the spectrum from 190 nm to 2000 nm.

4. Results and discussion

Figure 7 shows that variation of the driving voltage amplitude from 0 to 5 V at a frequency of 5 to 500 Hz provides four different colours, i.e. blue, green, yellow and red. Previously, only two (*19*) or three (*20*) colours were produced. The colours obtained have been characterised with spectroscopic data as well as microphotographs of textures, which are also shown in Figure 7. Figure 8 shows the corresponding chromaticity diagram expressed as a 1931 CIE chart for different voltages.

The contrast ratio of birefringence colours depends on the spectral range and on the frequency

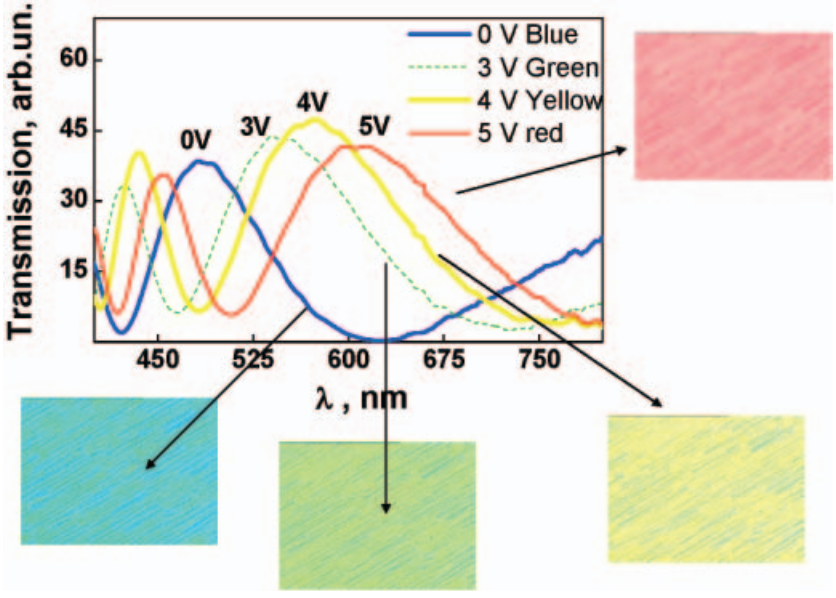

Figure 7. Light transmission spectra of 5 µm DHF cell placed between two crossed polarisers under an applied voltage of 0 V, 3 V, 4 V and 5 V. Helix pitch is <1 µm, unwinding voltage is 6 V, measured frequency of colour switch 100 Hz, horizontal size of microphotographs is 500 µm.

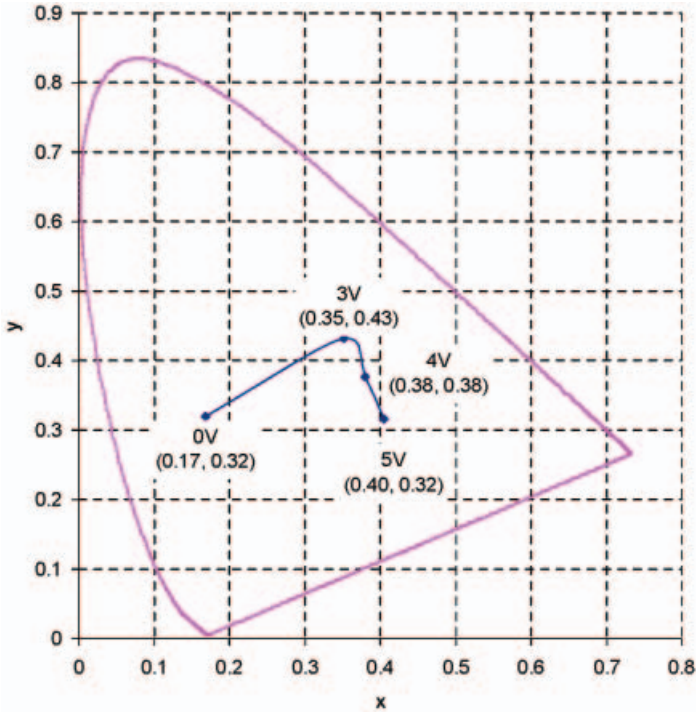

Figure 8. Colour obtained under different voltages expressed in a 1931 CIE chart using the data of Figure 7.

of colour switching. The maximum contrast obtained in our experiment was at 100 Hz and decreased on either side. Figure 9 shows the dependence of the contrast ratio as a function of frequency, which shows a high contrast for the red colour. Similarly, other colours show a reasonable contrast. It is interesting to note that the frequency range from 20 Hz to 100 Hz gives almost the same level of the contrast for different voltages.

The next step was to obtain the colours under driving voltage frequency variation at fixed voltage amplitude of 15 V. Figure 10 shows the transmission spectra for the five different colours (blue, aquamarine, green, yellow and red) obtained as a result of changing the driving voltage frequency.

Theoretical evaluation and experimental measurement of light transmission spectra at high frequency (10 kHz to 250 kHz) are in a good agreement

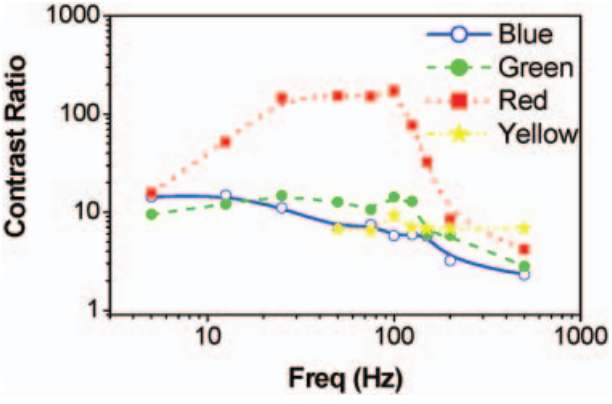

Figure 9. Contrast ratio of birefringence colours vs. the frequency of switching. Note that maximum contrast is obtained for red colour at 100 Hz, decreasing thereafter on both sides.

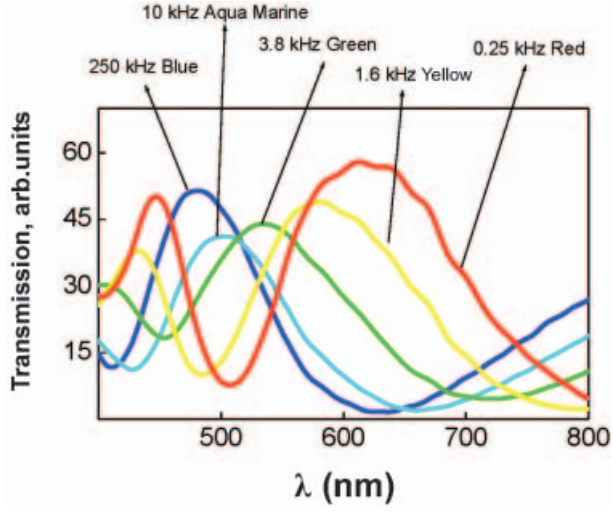

Figure 10. Light transmission spectra of 6 µm DHF cell placed between two crossed polarisers under applied frequencies of 250 kHz (blue), 10 kHz (aquamarine), 3.8 kHz (green), 1.6 kHz (yellow) and 0.25 kHz (red). Helix pitch <1 µm, measured at fixed voltage 15 V.

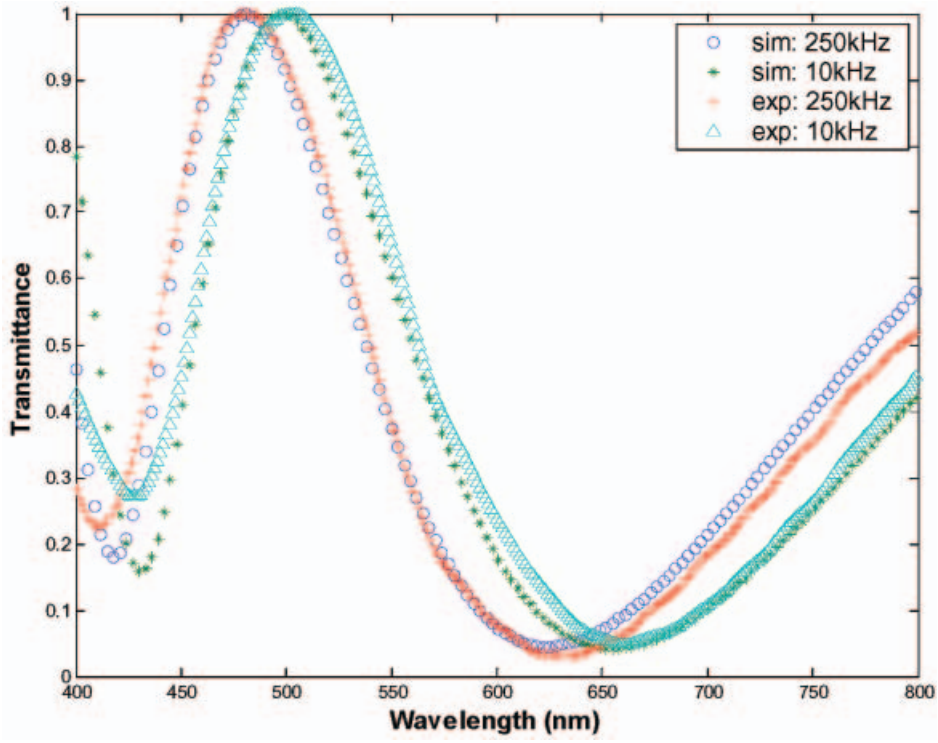

Figure 11. Comparison between simulated and measured spectra for high-frequency electric field.

(Figure 11) as soon as the condition provided by Equation (12) is valid.

Figure 12 shows the corresponding chromaticity diagrams expressed in a CIE chart for different frequency, emphasising the evidence of different colours.

Frequency-controlled birefringence colours were obtained in the high-frequency DHF mode (*27*),

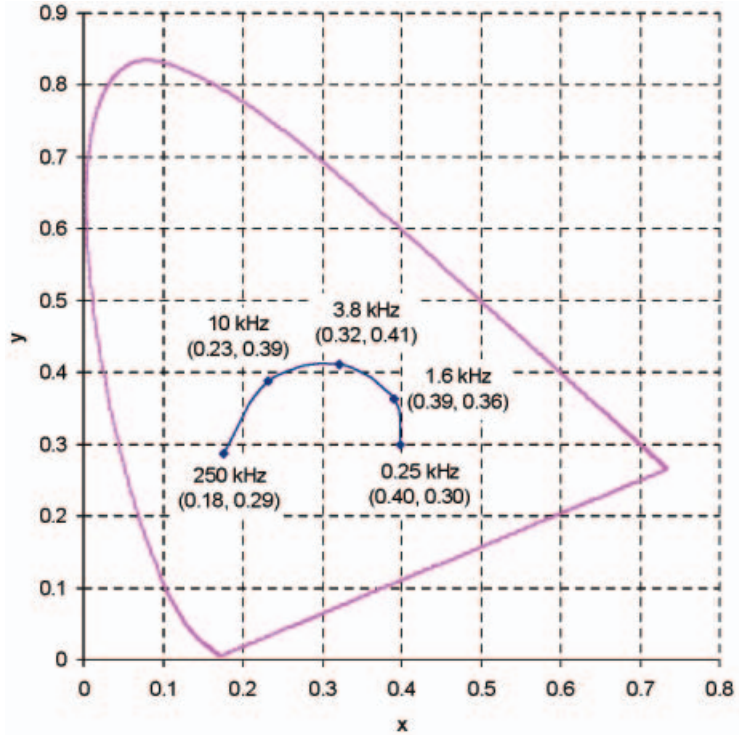

Figure 12. Colour obtained under different frequencies expressed in a 1931 CIE chart using the data of Figure 10.

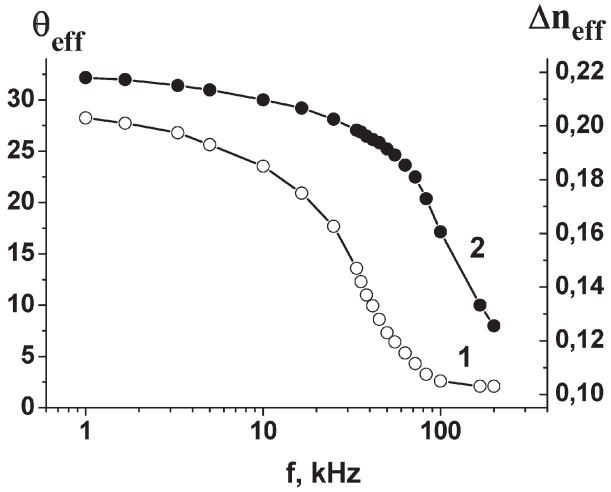

Figure 13. Frequency dependence of the apparent birefringence (curve 1) and apparent tilt angle (curve 2) in high-frequency DHF mode; the FLC layer thickness is 5 μm, T=23°C.

providing an electro-optical response time less than 1 μs, over a broad temperature range (about 60°C) and two variations of the apparent birefringence with driving voltage frequency from 1 kHz to 250 kHz (Figure 13).

The results presented in Figures 10 and 13 show a very promising behaviour of the high-frequency DHF mode in electrically controlled birefringent colour switching. Using this technique it should be possible to obtain field-sequential colour displays where a fast switching time is required.

5. Conclusions

Four colours with a change of driving voltage amplitude and five colours under driving voltage frequency variation have been obtained in deformed helix ferroelectric LC cells with the application of a relatively small electric field. These results can be helpful for fabricating field-sequential colour liquid crystal displays without colour filters. The DHF FLC cells exhibit fast switching time, which is required for this type of display.

Acknowledgements

This work was partly supported by HKUST grant CERG 612406 and Russian Foundation for Basic Research, grants 07-07-91582 and 08-03-90009-Bel_a.

References

(1) Takahashi T.; Furue H.; Shikada M.; Matsuda N.; Miyama T.; Kobayashi S. *Jap. J. Appl. Phys.* **1999**, *38*, L534–L536.
(2) Lee J.H.; Zhu X.; Wu S.T. *J. Display Technol.* **2007**, *3*, 2–8.
(3) Sun P.-L. *Proc. SPIE* **2008**, *6807*, 68070B-1–68070B-8.
(4) Gauza S.; Zhu X.; Piecek W.; Dabrowski R.; Wu S.T. *J. Display Technol.* **2007**, *3*, 250–252.
(5) Chen Y.F.; Chen C.-C.; Chen K.-H. *J. Display Technol.* **2007**, *3*, 377–385.
(6) Takatori K.; Imai H.; Asada H.; Imai M. *SID'01 Dig.* **2001**, 48–51.
(7) Xu P.; Li X.; Chigrinov V. *Eurodisp'05 Dig.* **2005**, 298–300.
(8) Pozhidaev E.; Chigrinov V.; Huang D.; Zhukov A.; Ho J.; Kwok H.S. *Jap. J. Appl. Phys.* **2004**, *43*, 5440–5446.
(9) Xu P.; Li X.; Chang W.S.; Chong C.S.; Wong K.Y.; Chigrinov V. *IDW'06* **2006**, 109–112.
(10) Meyer R.B.; Liebert L.; Strzelecki L.; Keller P. *J. Phys. Lett.* **1975**, *30*, 69.
(11) Beresnev L.A.; Chigrinov V.G.; Dergachev D.I.; Pozhidaev E.P.; Funfshilling J.; Schadt M. *Liq. Cryst.* **1989**, *5*, 1171–1177.
(12) Clark N.A.; Lagerwall S.T. *Appl. Phys. Lett.* **1980**, *36*, 899–901.
(13) Wand M.D.; Vohra R.; O'Callaghan M.; Roberts B.; Escher C. *SPIE Proc.* **1992**, *1665*, 176–183.
(14) Podgornov F.; Pozhidaev E.; Ganzke D.; Haase W. *Proc. IEEE* **2001**, 1004.
(15) Chigrinov V.G.; Pozhidaev E.P.; Yakovlev D.A.; Kwok H.S. *Proc. IEEE* **2003**, 204.
(16) Thakur A.K.; Kaur S.; Bawa S.S.; Biradar A.M. *Appl. Opt.* **2004**, *43*, 5614–5617.
(17) Jo J.S.; Ozaki M.; Yoshino K. *Jap. J. Appl. Phys.* **2003**, *42*, 526–530.
(18) Kaur S.; Thakur A.K.; Chauhan R.; Bawa S.S.; Biradar A.M. *J. Appl. Phys.* **2004**, *96*, 2547–2551.
(19) Abdulhalim I.; Moddel G. *Mol. Cryst. Liq. Cryst.* **1991**, *200*, 79–101.
(20) Kompanents S.I.; Pozhidaev E.P. *Ferroelectrics* **1998**, *214*, 93–100.
(21) Chigrinov V.G., *Liquid Crystal Devices: Physics and Applications;* Artech House, Boston: London (1999).
(22) Li X.H.; Murauski A.; Muravsky A.; Xu P.Z.; Cheung H.L.; Chigrinov V.G. *J. Display Technol.* **2007**, *3*, 273–279.
(23) Chigrinov V.; Prudnikova E.; Kozenkov V.; Kwok H.; Akiyama H.; Kawara T.; Takada H.; Takatsu H. *Liq. Cryst.* **2002**, *29*, 1321–1327.
(24) Pozhidaev E.; Chigrinov V.; Huang D.; Zhukov A. *Jap. J. Appl. Phys.* **2004**, *43*, 5440–5446.
(25) Huang D.D.; Pozhidaev E.; Chigrinov V.G.; Cheung H.L.; Ho Y.L.; Kwok H.S. *Displays* **2004**, *25*, 21–29.
(26) Huang D.D.; Pozhidaev E.; Chigrinov V.G.; Cheung H.L.; Ho Y.L.; Kwok H.S. *J. SID* **2004**, *12*, 455–459.
(27) Pozhidaev E.P.; Pikin S.A.; Ganzke D.; Shevtchenko S.A.; Haase W. *Ferroelectrics* **2000**, *246*, 235–245.